Hindawi
Wireless Communications and Mobile Computing
Volume 2018, Article ID 2408496, 10 pages
https://doi.org/10.1155/2018/2408496

Research Article

Compressed Detection for Pulse-Based Communications in the Terahertz Band

Pankaj Singh,[1] Byung-Wook Kim,[2] and Sung-Yoon Jung [1]

[1]*Department of Electronic Engineering, Yeungnam University, Gyeongbuk 38541, Republic of Korea*
[2]*Department of Information Communication Technology Automotive Engineering, Hoseo University, Chungcheongnam 31702, Republic of Korea*

Correspondence should be addressed to Sung-Yoon Jung; syjung@ynu.ac.kr

Received 14 March 2018; Revised 22 August 2018; Accepted 5 September 2018; Published 24 September 2018

Academic Editor: Pierre-Martin Tardif

Terahertz (THz) band (0.1-10 THz)-based electromagnetic communications are envisioned as a key technology to enable future high-data-rate short-range ultrabroadband communications. However, one of the fundamental bottlenecks is the efficiency of the analog-to-digital converters (ADCs) considering the formidable challenge of sampling the signal at the Nyquist rate eventually increasing transceiver design complexity. The Compressed sensing (CS) framework enables the successful reconstruction of sparse signals from a small set of projections onto a random vector which would lead to sub-Nyquist rate sampling. In this paper, THz band channel estimation based on the theory of CS is developed. The proposed approach exploits the fact that transmitting an ultrashort pulse through a multipath THz channel leads to a received THz signal that can be approximated by a linear combination of a few atoms from a predefined dictionary, yielding thus a sparse representation of the received signal. The fundamental idea is in the design of the dictionary of atoms that closely matches the transmitted pulse leading thus to a higher probability of CS reconstruction. The Orthogonal Matching Pursuit (OMP) algorithm is used to identify the strongest atoms in the projected signal. This reconstructed signal is subsequently used as a reference template in a correlator-based detector. The bit error rate (BER) performance of the proposed detector is analyzed and compared with the conventional CS-based channel estimation and reconstruction approach. Extensive simulations show that, for different design parameters, our proposed detector outperforms the traditional CS-based correlator receiver for the same sampling rate leading thus to a much-reduced use of analog-to-digital resources. Moreover, the proposed detector has been shown to reduce the hardware complexity of the receiver by significantly reducing the number of parallel mixer-integration branches.

1. Introduction

Wireless data communication is penetrating into many dimensions of human life, from mobile Internet to real-time healthcare monitoring and environmental protection. Moreover, wireless data traffic has been exponentially increasing which will lead to an increasing demand for the high-speed wireless communication, anywhere, anytime, in the near future. To satisfy the forthcoming data needs and develop future wireless communications systems, we need to utilize the already congested spectrum very efficiently. One of way is to improve our classical communication paradigms using more advanced digital schemes, e.g., Orthogonal Frequency Division Multiplexing (OFDM), Multiple-Input Multiple-Output (MIMO) systems, and beamforming. Another way is to look for the new solutions at the same time, e.g., cognitive radio and underutilized bands. Terahertz (THz) band is one such least explored zone of the electromagnetic (EM) spectrum. Recently, Terahertz band (0.1 THz–10.0 THz) communications are envisaged as a wireless technology that can bring novel solutions to the future communication needs, particularly in the Wireless Personal Area Networks (WPANs) [1]. Terahertz band-based short-range nanoscale communications would enable Terabit-per-second (Tbps) links in the short-range, i.e., up to 1 m [2]. The expected range of communication can be increased up to 10 m using the transparency windows achieving a capacity of up to 10 Mbps [3]. This would enable the next-generation small cell cellular networks with ultrahigh-speed data communication to alleviate the problem of spectrum scarcity and capacity

limitations. Moreover, THz band communications open the door to the development of variety of applications which demand ultrahigh data rates in many fields such as medical, environmental, and military [1].

However, there exist several research challenges from the communication perspective. One of the main problems is the high-frequency signal processing. Over the years, signal processing has been governed by classical Nyquist theorem. According to this theorem, a signal can be determined from its samples, if the sampling rate is more than twice the highest frequency present in the signal. In other words, the number of samples needed to reconstruct a signal depends on its bandwidth. However, due to the very short duration and ultrabroadband nature of the transmitted THz signals, this theorem imposes several challenges on the hardware, storage, and subsequent signal processing ultimately leading to stressed out analog-to-digital converters (ADCs) at the receiver side [4, 5]. Moreover, the state-of-the art ADCs can only sample at rates around 100 Giga-Samples-per-second (GSas) [6, 7], much below the Nyquist rate for THz signals. On the other hand, most of the signals with large bandwidth have a small rate of information [8]. In recent years, an alternative approach has emerged for signal reconstruction known as *compressed sensing* (CS) [9]. This method uses the sparse nature of wideband signals and provides an option to deal with the signal reconstruction problem by utilizing far fewer samples than required by the Nyquist theorem.

The field of CS has been heavily investigated in recent years for various communications systems. Different works on CS in combination with ultrawideband (UWB) related to channel estimation [10, 11], detection [12, 13], and time of arrival (ToA) estimation [14, 15] have been presented. At millimeter wave (mmWave) frequencies (30 GHz-300 GHz), an efficient channel estimator using CS for hybrid MIMO system has been proposed in [16]. An approach to leverage the sparse structure of the frequency-selective mmWave channels and a formulation for channel estimation has been developed in [17]. An adaptive one-bit compressed sensing scheme that can be used at low-resolution mmWave receivers for channel estimation has been proposed as an alternative to high-resolution power-hungry ADCs [18]. In the THz band, as of now, CS has been exploited for applications in the fields of Imaging and Spectroscopy [19]. However, in this work, CS has been analyzed from the wireless communications aspect in the Terahertz band.

In this study, mathematical properties of CS are applied to channel estimation and demodulation design for the pulse-based Terahertz band communications. In the THz band communications, an ultrashort femtosecond-long pulse is used as transmitted signal to convey the information [20]. The received signal remains sparse in time domain due to the multipath nature of the channel. Exploiting the signal sparsity of the received THz signals, a correlator-based detector based on the concept of CS has been developed. Using the frame template reconstruction of pilot symbols which has been done using the Orthogonal Matching Pursuit (OMP), the remaining information-bearing symbols are demodulated in the analog domain. The compressive measurements are sampled at the frame rate. Moreover, a new method, where measurements from all the frames are applied simultaneously to OMP, is also proposed. The proposed method exploits the received signal properties to design the dictionary of parameterized waveforms (atoms). As those waveforms closely match the remaining information carrying pulse, the new method has been shown to improve the receiver performance and reduce the hardware complexity at the same time.

The rest of this paper is organized as follows. In Section 2, basic theory related to CS has been discussed. Section 3 describes the system model for pulse-based Terahertz band communications including the multipath channel. In Section 4, the proposed CS-based channel estimation along with the corresponding demodulation scheme has been developed. A correlation-based detector has been used. In addition, the conventional CS-based scheme is also described. Section 5 shows the simulation results and the work is concluded in Section 6.

2. CS Preliminary

Compressed sensing is a novel mathematical concept, which provides an alternative to the existing state-of-the-art receivers which require extremely high-sampling rates for signal reconstruction [21–23]. Essentially, CS is signal reconstruction from random projections of a signal vector, provided that the signal is sparse in the vector space. Specifically, one can recover certain signals from far fewer samples than traditionally required. However, two important criteria must be satisfied for the successful reconstruction of the signal. First, the signal should be *sparse* in some domain. *Sparsity* implies that the signal has a few nonzero components on some basis. In other words, sparsity is a signal property that measures the signal redundancy in some domain or basis. If a signal has only "K" nonzero coefficients on an adequately chosen basis, it is said to be K-sparse. The second criterion is that the property of *incoherence* must be satisfied. Incoherence measures the maximum correlation between any two elements of two different matrices. These two matrices represent two different bases. If Φ is an $N \times N$ matrix representing the basis in which the signal is sparse and Ψ is an $M \times N$ measurement matrix, i.e., matrix used to sample or sense signal, then the property of incoherence between above two matrices translates to fewer samples requirement for the signal reconstruction.

Mathematically, if a signal, $x \in \mathbb{R}^N$, composed of N samples is K-sparse in some orthonormal basis, $\Phi = [\phi_1, \phi_2, \ldots, \phi_N]$, such that x can be approximated by a linear combination of K-vectors from the dictionary Φ, where $K \ll N$, then the CS theory shows that x can be recovered from $M(\ll N)$ measurements with high probability when $M = CK \log N$, where C is the oversampling factor [21]. The measurements are given by $y = \Psi x$, where Ψ is a $M \times N$ random projection matrix. At the same time, to satisfy the incoherence property between sensing matrix and the representation matrix, random matrices are proposed as they are largely incoherent with any fixed basis. The Restricted Isometry Property (RIP) criterion is the most widely used tool to check whether a specific sensing matrix is qualified for recovering a sparse signal or not. A matrix Ψ, of size $M \times N$,

Table 1: Orthogonal matching pursuit algorithm.

Step 1	**Input:** y and Ψ
	Initialize: $r_0 = y$, $\hat{x}^0 = 0$, $T_0 = \emptyset$
Step 2	**for** $i = 1; i := i + 1$ till stopping criteria is met **do**
	$m^i = \Psi^\top r_{i-1}$
	$n_i = \arg\max_n \lvert m_n^i \rvert / \lvert\lvert \psi_n \rvert\rvert_1$
	$T_i = T_{i-1} \cup n_i$
Step 3	$\hat{x}_{T_i}^i = (\Psi(T_i)^\top \Psi(T_i))^{-1} \Psi(T_i)^\top y$,
	$r_i = y - \Psi \hat{x}^i$
Step 4	**end for**
	Output: r_i and $\hat{x}^i$

is said to satisfy RIP of order K with a restricted isometry constant (RIC), with $\delta_K \in (0, 1)$ being the smallest number such that

$$\left(1 - \delta_K\right) \|x\|_2^2 \leq \|\Psi x\|_2^2 \leq \left(1 + \delta_K\right) \|x\|_2^2 \tag{1}$$

holds for all K-sparse vectors x. In other words, it could be loosely said that a matrix Ψ obeys the RIP of order K if δ_K is not too close to one. RIP of order K implies that Ψ preserves the Euclidean distance between any two K-sparse signals which in turn implies that K-sparse vectors cannot reside in the null space of Ψ. A random $M \times N$ matrix whose entries are independently identically distributed (i.i.d.) realization of certain zero-mean random variable with variance $1/N$ satisfies the RIP with a high probability when $M \geq CK \log(N/K)$.

Regarding signal recovery, Orthogonal Matching Pursuit (OMP) [24] has been used as it is not based on optimization and finds the solution in an iterative fashion. It is faster and easier to apply as the number of iterations depends on the dimension of Ψ and it is quite transparent. The OMP algorithm finds the component with maximum correlation in the measurement signal, eliminates it from the signal, and searches again for the maximum correlation component in the residual signal (Table 1). In particular, the approximation for x is updated in each iteration by projecting y orthogonally on the columns of Ψ associated with the current support set T_i. Therefore, OMP minimizes $\|y - \Psi\hat{x}\|_1$ over all $\hat{x}$ with support T_i. Note that the minimization is performed with respect to all the currently selected coefficients as

$$\hat{x}_{T_i}^i = \arg\min \left\| y - \Psi \hat{x} \right\|_1^2 \tag{2}$$

The OMP algorithm runs as follows:

(1) Initialize the residual measurement $r_0 = y$, the approximation $\hat{x}^0 = 0$, where $\hat{x}^i \in \mathbb{R}^N$, and set $T_0 = \emptyset$. Let the iteration counter be $i = 1$.

(2) Solve the maximization problem $n_i = \arg\max_n \lvert m_n^i \rvert / \|\psi_n\|_1$, and update $T_i = T_{i-1} \cup n_i$.

(3) Solve the least square problem, $\hat{x}_{T_i}^i = (\Psi(T_i)^\top \Psi(T_i))^{-1} \Psi(T_i)^\top y$, and update $r_i = y - \Psi \hat{x}^i$, where $\Psi(T_i) = \{\psi_t \mid t \in T_i\}$.

(4) If the stopping criterion is satisfied, stop; otherwise $i = i + 1$ and return to step (2).

3. CS-Based Pulsed THz Band Communications

In the CS framework, a set of pilot signals are used to estimate the channel. In other words, reference template reconstruction is performed which is then used for subsequent correlation detection [10, 25, 26].

3.1. Transmitted Signal Model. In the THz band communications, information symbols are conveyed by a stream of ultrashort femtosecond-long pulses [20]. The symbol structure is shown in Figure 1. A symbol duration consists of several numbers of frames (N_f), each having a duration of T_f. Each frame has a pulse of ultrashort duration, T_p. The transmitted signal, $s(t)$, can be represented as

$$\begin{aligned} s(t) = &\sum_{i=0}^{N_p-1} \sum_{m=0}^{N_f-1} p\left(t - iN_fT_f - mT_f\right) \\ &+ \sum_{j=0}^{N_i-1} a_j \sum_{n=0}^{N_f-1} p\left(t - jN_fT_f - nT_f - N_pN_fT_f\right), \end{aligned} \tag{3}$$

where $t \in [0, T_s]$, $T_s (= N_sN_fT_f)$ is the symbol duration, $p(t)$ is the first-order Gaussian derivative pulse, $a_j \in \{\pm 1\}$ is the binary modulated information symbols, N_p is the total number of unmodulated pilot symbols, N_i is total number of information symbols, and $N_s (= N_p + N_i)$ is the total number of symbols.

As shown in Figure 1, the signaling scheme is based on pilot symbol aided modulation. Each signaling includes the N_p pilot symbols, which are not data modulated, and $N_i (= N_s - N_p)$ data modulated symbols. The pilot symbols are used for channel estimation. In addition, the transmitted pulse is the first derivative of the Gaussian given by

$$p(t) = -\frac{k(t-\mu)}{\sqrt{2\pi}\sigma^3} \exp\left(-\frac{(t-\mu)^2}{2\sigma^2}\right), \tag{4}$$

where k is the normalization factor, μ is the mean of the Gaussian pulse, and σ is the root mean square (RMS) width of the pulse.

3.2. Channel Model. The Terahertz channel has very-high spreading loss and molecular absorption loss unlike other frequency bands [20, 27]. The absorption loss depends on the concentration of gaseous molecules present in the propagation medium, mainly water vapor molecules. It results in the strong dependence of Terahertz band on the signal frequency, transmission distance, and propagation medium characteristics. For short range, THz band offers incredibly huge bandwidth (almost 10 THz wide window). In addition, the multipath propagation results in very-high reflection losses which depend on the shape, material, and roughness of the reflecting surface affecting the Terahertz wave propagation [28]. For instance, surfaces considered as smooth at lower-frequencies becomes rough at Terahertz frequencies. This is because the level of roughness increases as the wavelength decreases. Moreover, the reflection losses also depend on the incident angles of the reflected waves [29].

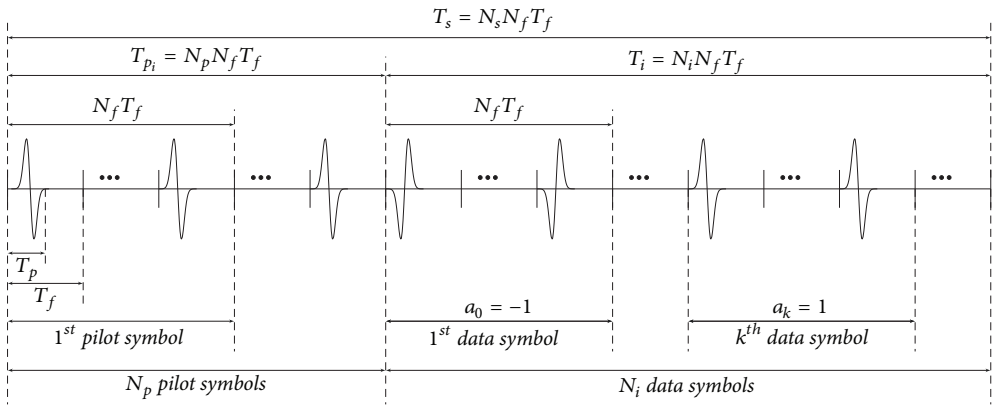

Figure 1: Transmitted signaling structure.

A simple multipath channel model for the Terahertz band can be given by the following impulse response [28, 29]:

$$h(t) = \mathcal{F}^{-1}\left[H_{eq}(f,d,r)\right], \tag{5}$$

with

$$H_{eq}(f,d,r) = H_{LoS}(f,d) + \sum_{i=1}^{L} H_{NLoS,i}(f,r_i), \tag{6}$$

where $\mathcal{F}^{-1}[.]$ is inverse Fourier transform operation, H_{eq} represents the equivalent channel transfer function which is a combination of line-of-sight (LoS) (i.e., H_{LoS}) and i-th non-line-of-sight (NLoS) path's (i.e., $H_{NLoS,i}$) channel transfer function [28, 29], L is the total number of indirect rays, d is the LoS distance, r_i denotes the NLoS distance of the i-th path between the transmitter and receiver, and f is frequency. Moreover, the LoS and NLoS transfer functions can be written as follows [28, 30]:

$$H_{LoS}(f,d) = H_{spr}(f,d)\, H_{abs}(f,d)\, e^{-j2\pi f \tau_{LoS}} \tag{7}$$

and

$$H_{NLoS,i}(f,r_i) = H_{spr,i}(f,r_i)\, H_{abs,i}(f,r_i)\, e^{-j2\pi f \tau_{NLoS_i}}, \tag{8}$$

where H_{spr} and H_{abs} are the spreading loss and molecular absorption loss transfer functions [28, 29], respectively, and τ_{LoS} and τ_{NLoS_i} are the propagation delays of the LoS path and the i-th NLoS path, respectively. Figure 2 depicts the Terahertz band path gain model as a function of frequency for various distances. As we can see, for larger distances, various spikes of attenuation occur in the path gain model due to the molecular absorption loss.

3.3. Received Signal. After passing through the channel, the received signal can be given as

$$r(t) = s(t) * h(t) + n(t), \tag{9}$$

where $n(t)$ is the THz band noise comprising molecular absorption noise [27] and additive white Gaussian noise (AWGN). The received signal in (9) can be expanded as

$$\begin{aligned} r(t) &= \sum_{i=0}^{N_p-1}\sum_{m=0}^{N_f-1} p_r\left(t - iN_fT_f - mT_f\right) \\ &\quad + \sum_{j=0}^{N_i-1} a_j \sum_{n=0}^{N_f-1} p_r\left(t - jN_fT_f - nT_f - N_pN_fT_f\right) \\ &\quad + n(t), \end{aligned} \tag{10}$$

where $p_r(t)(= p(t) * h(t))$ is the noiseless composite pulse-multipath channel.

4. CS-Based Correlator Detector

In this section, we propose a simplified correlator-based detector for the THz band communications. The received signal per frame is correlated with a reference template to decode the transmitted information symbol in the corresponding frame. The reference template is the pulse-multipath frame template that is reconstructed using compressed sensing. Therefore, the receiver performs frame-rate sampling on the correlator output to generate sufficient statistics for the detection of the transmitted information symbol. The proposed correlator-based detector is implemented in the analog domain (cf. Figure 3). As shown, the first stage is the channel estimation stage and the next stage is the demodulation stage. In the channel estimation stage, based on the received pilot waveforms, the frame-long channel reference template is reconstructed. Let $r_p(t)$ be the pilot signal carrying N_p pilot symbols with N_f frames in each corresponding symbol. Thus, $r_p(t)$ can be represented as

$$r_p(t) = \sum_{i=0}^{N_p-1}\sum_{m=0}^{N_f-1} p_r\left(t - iN_fT_f - mT_f\right) + n(t), \tag{11}$$

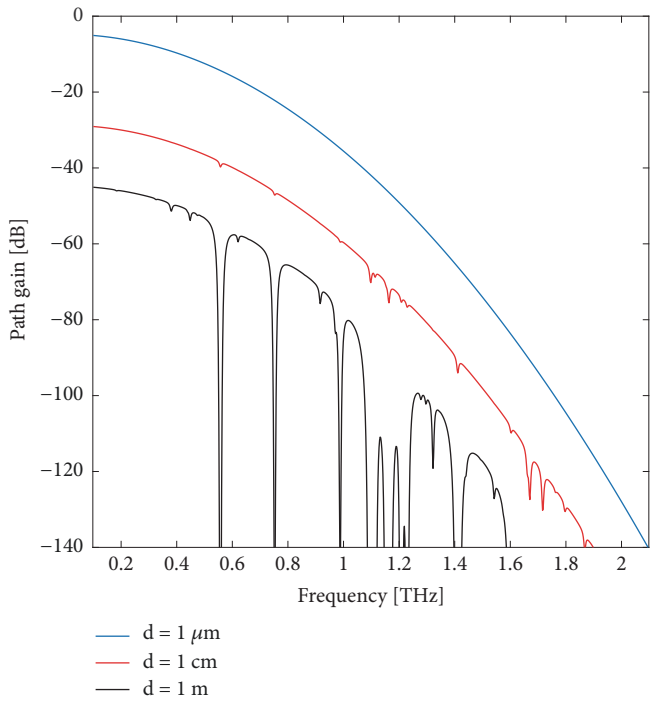

FIGURE 2: THz band path gain as a function of frequency for various distances.

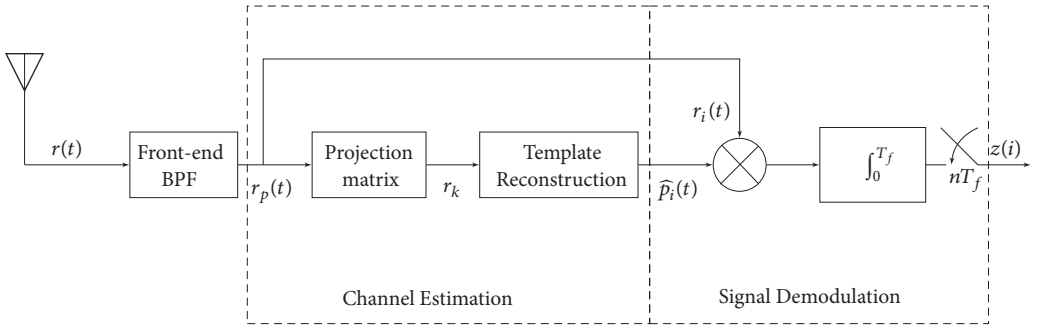

FIGURE 3: Block diagram of proposed CS correlator-based detector.

where $t \in [0, T_{p_i})$. Considering that the received signal is observed over nonoverlapping time intervals in the time window frame of $t \in [kT_f, (k+1)T_f)$ for $k = 0, 1, 2, \ldots, N_f N_p - 1$, and assuming perfect timing synchronization, each time interval (i.e., T_f) contains multipath frames contaminated with noise. Therefore, the received pilot symbol per frame can be represented as

$$g_k(t) = \left\lfloor \frac{k}{N_f} \right\rfloor p_r(t) + n(t), \tag{12}$$

where $g_k(t)$ is frame long received pilot symbol. In the next subsections, we develop the channel estimation model for both conventional and proposed CS-based correlation receivers that finally lead us to the demodulation stage.

4.1. Conventional CS-Based Channel Estimation. The channel estimation procedure is as follows. First, the compressed samples are taken at frame-rate sampling in the receiver. Second, using OMP, original pulse-multipath channel frame is reconstructed from less number of samples. Exploiting the time sparsity nature of the Terahertz channel, the representation (basis) matrix Φ can be assumed to be an identity matrix [10]. The input to the channel estimation block (i.e., $r_p(t)$) is an analog multipath frame of each pilot symbol and the output (i.e., $\boldsymbol{p_i}$) is a discrete representation of analog multipath frame (cf. Figure 3). In other words, as the received signal is composed of time-shifted versions of multipath template contaminated with noise, by observing the signal in a frame-long interval, and randomly projecting the observed signal, a noisy template can be recovered using OMP algorithm.

The discrete-time representation of the continuous multipath frame in each pilot symbol is presented as $\boldsymbol{g_k} = [g_k(0), g_k(T), \ldots, g_k((N-1)T)]^\top$, where N is the number of samples and T is the Nyquist sampling period. The

elements of the measurement matrix, $\Psi_{M\times N}$, can be chosen as independent and identically distributed (i.i.d.) Gaussian random variables with zero mean and $1/N$ variance. If the sparsity order of the pulse-multipath frame is given by K, the number of required samples to fulfill the RIP condition and incoherence property is given by

$$M \geq CK \log_{10}\left(\frac{N}{K}\right), \tag{13}$$

where $C(\geq 1)$ is the oversampling factor. Compressed sensing based sampling equation for the k-th frame can be written as

$$\boldsymbol{r_k} = \Psi \boldsymbol{g_k}, \tag{14}$$

where $\boldsymbol{r_k} = [r_k(0), r_k(1), \ldots, r_k(M-1)]^\top$. Since N_pN_f pilot waveforms are used for channel estimation, the estimated composite pulse-multipath channel is formed by averaging over N_pN_f noisy templates. In other words, the random projected signals corresponding to the received pilot waveforms are averaged and input to the OMP algorithm.

As the random projected signals are averaged before reconstruction to obtain the discrete-time channel template, $\boldsymbol{p_i}$, the sampled vector $\boldsymbol{r}$ is given by

$$\boldsymbol{r} = \frac{1}{N_pN_f} \sum_{k=0}^{N_fN_p-1} \boldsymbol{r_k}. \tag{15}$$

Finally, $\boldsymbol{p_i}$ is recovered using the following objective function given by

$$\begin{aligned} \boldsymbol{p_i} = \min \quad & \|\boldsymbol{g_k}\|_1 \\ \text{s.t.} \quad & \boldsymbol{r} = \Psi \boldsymbol{g_k}, \end{aligned} \tag{16}$$

where $\boldsymbol{p_i} = [p_i(0), p_i(1), \ldots, p_i(N-1)]^\top$. Note that the above method is computationally less expensive compared to reconstructing every frame. This is because by using OMP first and then averaging over the N_pN_f samples, it requires running the OMP only once. Moreover, it implicitly mitigates the effect of noise. The reconstructed pulse-multipath frame template is now used to demodulate the remaining information-bearing symbols.

4.2. Proposed CS-Based Channel Estimation. In the conventional method, ensemble of projected samples from pilot symbol is collected and the multipath frame template is then reconstructed after ensemble averaging over N_f frames. However, the number of projected measurement samples is usually found to be very large. For instance, if the composite pulse-multipath channel frame is composed of $N = 256$ samples, then, with a sparsity order of 35% and $C = 1$, the minimum value of projected samples, i.e., M_{min}, is 40. In other words, the pulse-multipath channel template could be reconstructed with at least 40 random measurements. This will result in 40 numbers of correlator branches at the receiver, which may increase hardware cost. Therefore, we propose a new template reconstruction mechanism which significantly reduces the number of correlator branches (i.e., M) and also improves the performance of the system simultaneously.

The proposed reconstruction method exploits the unique symbol structure of the Terahertz band symbols. First, a THz symbol consists of a number of frames, and each frame carries a pulse. Therefore, the received signal is formed by scaled and delayed versions of the transmitted pulse. Since the dictionary should contain elements (atoms) that can fully represent the information carrying symbols, the elements of dictionary are generated so that they closely relate to the pulse waveform. Therefore, the atoms in the dictionary are thus delayed versions of the THz transmitted pulse. Second, the same frame is repeated over the entire pilot symbol duration (i.e., T_{p_i}). In other words, the frames carry the same information every T_f period. Therefore, it is not necessary to take the M_{min} number of samples every frame. Instead, a much lower number of samples per frame can be used as all the frames carry the same information. Therefore, by collecting samples from each frame, we can create a sequence of random vectors. In other words, the proposed method collects $M(\ll M_{min})$ measurement samples from each frame to finally create a random vector before template reconstruction. As we collect much lower number of samples per frame, the required number of correlator branches decreases accordingly. Moreover, as the total number of samples for template reconstruction increases, the performance of the proposed scheme improves.

Now, the received pilot waveform per frame is given by (12). The measurement matrix is chosen to be i.i.d. with Gaussian random variables having zero mean and $1/N$ variance. Each frame is sampled by a different Ψ (cf. Figure 4). Therefore, for k-th frame, Ψ_k can be attributed as a measurement matrix with the dimension $M \times N$. Therefore, the CS operation over k-th frame is given by

$$\boldsymbol{r_k} = \Psi_k \boldsymbol{g_k}. \tag{17}$$

Then, the collected samples from each frame are stored as another vector given by

$$\boldsymbol{r} = \left[\boldsymbol{r_1}^\top, \boldsymbol{r_2}^\top, \ldots, \boldsymbol{r_k}^\top, \ldots, \boldsymbol{r_{N_fN_p}}^\top\right]^\top, \tag{18}$$

where $\boldsymbol{r_k}^\top$ is the transpose of the vector $\boldsymbol{r_k}$ given by (14). Similarly, the actual reconstruction matrix (i.e., $\boldsymbol{V}$) is formed by collecting the measurement matrix used for each frame as

$$\boldsymbol{V} = \left[\Psi_1, \Psi_2, \ldots, \Psi_k, \ldots, \Psi_{N_pN_f}\right]^\top. \tag{19}$$

Finally, the objective function for template reconstruction is again based on l_1-norm optimization process as

$$\begin{aligned} \boldsymbol{p_i} = \min \quad & \|\boldsymbol{g_k}\|_1 \\ \text{s.t.} \quad & \boldsymbol{r} = \boldsymbol{V}\boldsymbol{g_k}. \end{aligned} \tag{20}$$

Similar to the conventional scheme, we used OMP algorithm for the reconstruction process.

4.3. Signal Demodulation. After the pulse-multipath frame template reconstruction, the template is used to demodulate

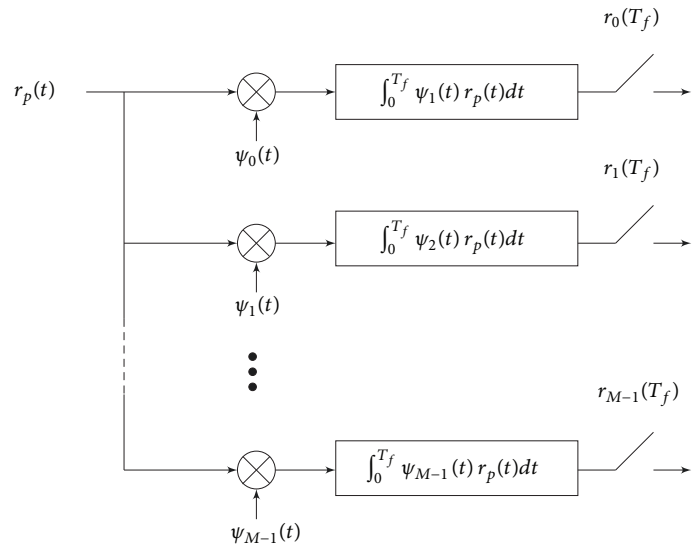

FIGURE 4: Proposed CS-based template reconstruction for a single frame.

the analog information-bearing signal at frame rate using the proposed CS correlator-based demodulation. The discrete form of multipath frame template can be approximated as

$$\widehat{p}_i(t) = \sum_{n=0}^{N-1} p_i[n]\, \mathrm{sinc}\left(\frac{t}{T} - n\right), \tag{21}$$

where $\widehat{p}_i(t)$ is the analog approximation of discrete multipath frame $p_i[n]$. Now, using $\widehat{p}_i(t)$, the information-bearing symbols (i.e., $r_i(t)$) can be demodulated. As each symbol consists of N_f frames, thus the decision statistic is given by adding N_f correlator output samples for the i-th symbol as

$$z(i) = \sum_{j=0}^{N_f-1} \int_{jT_f+iT_s}^{(j+1)T_f+iT_s} r_i(t)\, \widehat{p}_i\left(t - jT_f - iT_s\right) dt. \tag{22}$$

Eventually, the detected symbol is given by

$$\widehat{a}_i = \mathrm{sgn}\left(z(i)\right), \tag{23}$$

where sgn is a signum function.

5. Simulation Results

5.1. Performance Comparison. In this section, we compare the performance of the proposed correlator detector for two CS-based channel estimation schemes described above. Table 2 enlists the default simulation parameters unless otherwise mentioned. Average bit error rate (BER) is used as a performance criterion with respect to signal-to-noise ratio (SNR). In the simulation, binary pulse amplitude modulation is used for the information-bearing symbols where the information bits are independent binary symbols with equal probability. The Gaussian monocycle pulse is used for both the pilot and information-bearing symbols. For simplicity, the single-user peer-to-peer communication system and one pulse per frame are considered. The Terahertz channel has been assumed to be concentrated with 10% water vapor molecules. To avoid temporal broadening which causes interframe interference (IFI) and intersymbol interference (ISI), it is assumed that $T_f \gg T_p + \tau_{max}$, where τ_{max} is the maximum excess delay of the multipath channel. The maximal delay spread of the channel is 3.22 ps. As the total number of samples per pulse-multipath frame is N, and the actual number of random projections is given by M; the M/N ratio indicates the reduction in the number of samples used to reconstruct pulse-multipath frame. Furthermore, the maximum number of OMP iterations is set to 300 for the target residual energy of 10^{-4}.

TABLE 2: Simulation parameters.

Parameter	Values
Pulse width parameter (σ)	100 fs
Pulse duration (T_p)	0.6 ps
Frame duration (T_f)	200 ps
Number of frames (N_f) per symbol	5
Total symbol duration (T_s)	1 ns
Number of pilot symbols per signal (N_p)	1
Number of information symbols per signal (N_i)	1000
Number of samples per pulse-multipath frame (N)	350
Sparsity order (K)	35%
Number of Monte Carlo runs	10^4
Distance between nanomachines	0.5 mm

Figure 5 depicts BER performance of the CS correlator for different number of compressive measurements or random projections (i.e., M) given by M/N ratio. When $M/N = 0.1$, the number of compressive measurements is 10% of the pulse-multipath frame length. It can be seen that the proposed method outperforms the conventional method of CS-based reconstruction. This is because of the following two reasons. First is the design of a suitable dictionary to represent

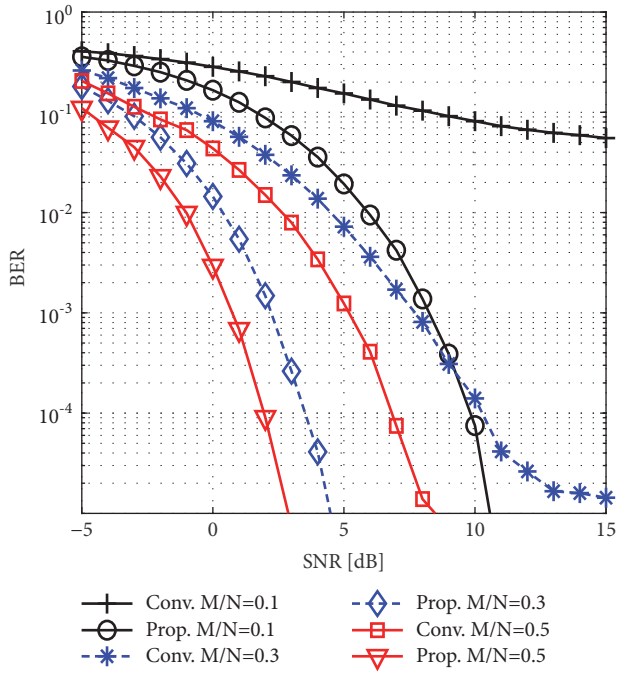

Figure 5: BER performance for different number of random projections.

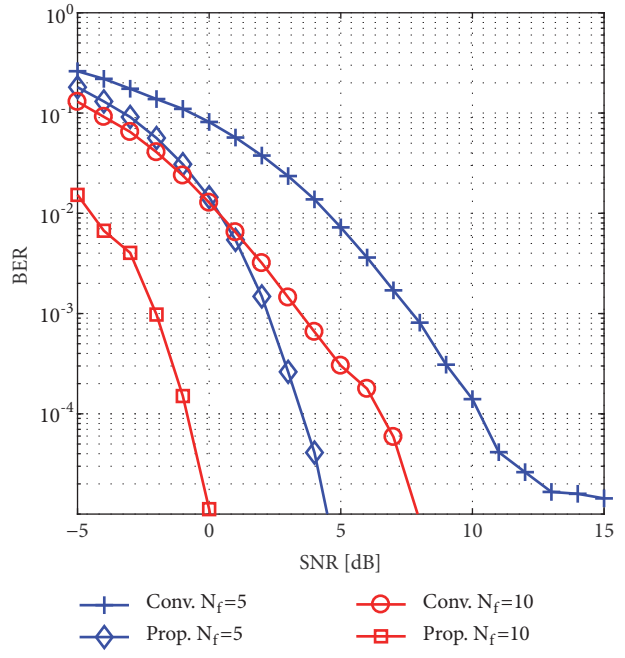

Figure 6: BER performance for different number of frames (N_h), with $M/N = 0.30$ and $N_p = 1$.

the THz signal. Second, the number of samples in the proposed method is increased to MN_f by stacking M samples for N_f frame. However, in the conventional method, we input only M samples to the OMP algorithm for the reconstruction. Therefore, even for the lower compression, the proposed method successfully estimates the channel pulse-multipath

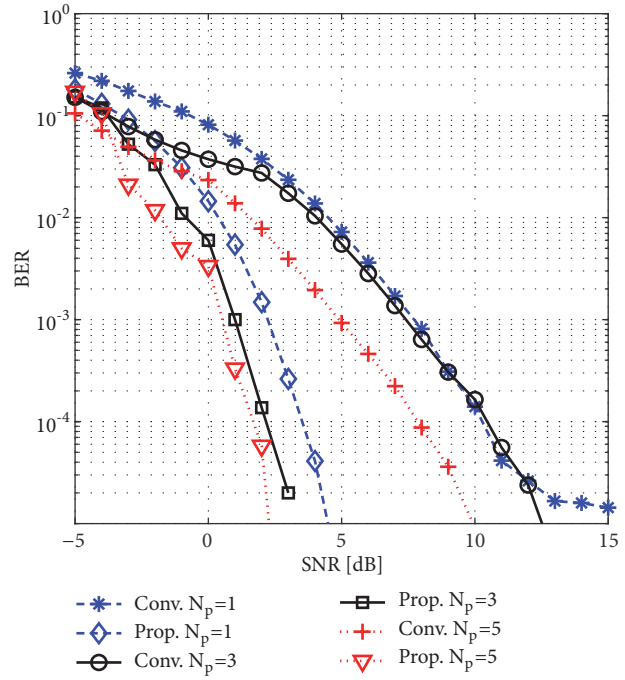

Figure 7: BER performance for different number of pilot symbols (N_p), with $M/N = 0.30$ and $N_h = 5$.

frame. We can observe that using the proposed CS-based channel estimation, by sampling the signal at 10% of the signal's sampling rate, similar performance could be achieved while sampling at 30% rate using conventional CS. Moreover, as expected, increase in the number of projections results in better BER even in low SNR region.

Figure 6 depicts the performance of the proposed detector for both schemes and different number of frames (i.e., N_f) per symbol. The M/N ratio is kept fixed at 0.30. It can be observed that as the frame size increases, BER performance is enhanced. This is because the increase in number of frames per symbol leads to decrease in noise in the correlator. However, with increasing frame size, the data rate would decrease. Therefore, for the same hardware complexity, by increasing the number of frames per symbol, better performance could be achieved. Moreover, our proposed scheme performs better than the conventional channel estimation scheme. We can observe that the performance gap in BER also depends on the number of frames. This is because even if the number of projections (i.e., M) is low, by having more number of frames, the total number of projections increases because of the stacking process. Hence, the performance gap is significant for the case of $N_f = 10$, particularly in the low SNR region. Furthermore, as expected, with increasing SNR, the performance difference between the conventional and the proposed schemes increases.

Figure 7 depicts the performance of the proposed scheme for different number of pilot symbols (i.e., N_p) per signal. The M/N ratio is kept fixed at 0.30 and the N_h is 5. We can observe that the proposed CS-based channel estimation scheme performs better than the conventional CS-based scheme. This is because of the design of the parameterized waveforms of

dictionary that closely resembles the information carrying pulses. However, we can observe that there is no significant performance gap between various values of N_p, particularly in the proposed scheme. This almost similar performance is because our proposed scheme is not able to exploit the stacking process as the number of frames in every pilot symbol remains the same. However, transmitting more pilot symbols per burst helps in reducing the noise component at the correlator resulting in minor improved performances.

5.2. Complexity Comparisons

5.2.1. Hardware Complexity. Needless to say, as CS-based approach performs template reconstruction from the randomly projected signals sampled at significantly reduced rate; it avoids the use of analog delay units needed in the implementation of conventional analog template-estimate approaches [25, 26]. In addition, the proposed CS-based scheme also reduces the hardware complexity of the conventional CS-based channel estimation scheme. This is given by the reduction in the number of parallel integrator-mixer branches (cf. Figure 3). For instance, considering the sparsity order of 35% (Table 2), using the conventional method (12), the minimum number of parallel branches (i.e., M_{min}) comes out to be approximately 56. However, using the proposed scheme, we can stack the M values from N_f frames before feeding it to the OMP algorithm. Therefore, if we stack $M = 12$ samples per frame, we can easily get 60 samples at the end (i.e., $MN_f = 60$), which is more than 56, thus satisfying the CS criteria easily. At the same time, we only need 12 parallel mixer-integration branches. This is almost 78% reduction leading to the lower cost and complexity at the receiver end.

5.2.2. Algorithm Complexity. In the proposed scheme, the program complexity is mainly driven by the complexity of the OMP algorithm. The OMP algorithm is used to solve the optimization problem mentioned in (16) and (20). OMP tries to recover the signal by finding the strongest component (atom) in the measurement signal, eliminating it from the signal, and searching again the dictionary for the strongest atom that is present in the residual signal. The computational cost of OMP is dominated by the matrix-vector products. As OMP limits the number of iterations by orthogonalizing the nonselected dictionary vectors (atoms) against those already selected, the algorithm converges in at most M iterations. However, it requires the additional computational cost of orthogonalization at each iteration. The running time of OMP is dominated by step 2 (Table 1), whose total cost is $O(CK^2N)$. The least square problem in step 3 is solved using Cholesky decomposition. At iteration i, OMP uses back-substitution to find the least-squares solution with a complexity of $O(i^2)$, where i is the number of iterations. Finally, the residual signal is computed with a cost of $O(Mi)$. Thus, the total complexity of the i-th iteration is $O(CK^2N + Mi + i^2)$. The storage price in the OMP algorithm is paid for the storage of the matrix Ψ which is of size $M \times N$ and the storage of Gramian matrix during Cholesky decomposition. Therefore, the storage cost for OMP is given as $O(KN \log N)$.

6. Conclusions

In this paper, we propose a new Terahertz band channel estimation and signal detection approach based on the theory of compressed sensing. The compressive detector exploits the signal sparsity model explicitly. A reduced number of random projections of the received ultrabroadband signal were used for signal reconstruction. Simulation results showed that the proposed detector outperforms the conventional compressive detector that does not exploit the unique symbol structure. In the viewpoint of hardware design, the proposed CS-based channel estimation leads to simplified receiver design comparatively. With far fewer measurements, the proposed receiver could be a significant step forward for using the compressive sensing as an alternative solution to the conventional receivers particularly in the ultrabroadband communication systems.

Data Availability

The simulation parameters data used to support the findings of this study are included within the article.

Conflicts of Interest

The authors declare that they have no conflicts of interest.

Acknowledgments

This work was supported by Basic Science Research Program through the National Research Foundation of Korea (NRF) funded by the Ministry of Education (NRF-2018R1A2B6002204).

References

[1] I. F. Akyildiz, J. M. Jornet, and C. Han, "Terahertz band: next frontier for wireless communications," *Physical Communication*, vol. 12, pp. 16–32, 2014.

[2] I. F. Akyildiz, F. Brunetti, and C. Blázquez, "Nanonetworks: A new communication paradigm," *Computer Networks*, vol. 52, no. 12, pp. 2260–2279, 2008.

[3] P. Boronin, V. Petrov, D. Moltchanov, Y. Koucheryavy, and J. M. Jornet, "Capacity and throughput analysis of nanoscale machine communication through transparency windows in the terahertz band," *Nano Communication Networks*, vol. 5, no. 3, pp. 72–82, 2014.

[4] A. Inamdar, A. Sahu, J. Ren, S. Setoodeh, R. Mansour, and D. Gupta, "Design and evaluation of flash ADC," *IEEE Transactions on Applied Superconductivity*, vol. 25, no. 3, 2015.

[5] V. de Araujo, E. Simas Filho, A. Oliveira, W. de Oliveira, and L. Esteves, "Integrated circuit for real-time poly-phase power quality monitoring," *Microelectronics Journal*, vol. 79, pp. 57–63, 2018.

[6] L. Kull, J. Pliva, T. Toifl et al., "Implementation of low-power 6-8 b 30-90 GS/s time-interleaved ADCs with optimized input bandwidth in 32 nm CMOS," *IEEE Journal of Solid-State Circuits*, vol. 51, no. 3, pp. 636–648, 2016.

[7] L. Kull, D. Luu, P. A. Francese et al., "CMOS ADCs Towards 100 GS/s and beyond," in *Proceedings of the 2016 IEEE Compound Semiconductor Integrated Circuit Symposium, CSICS 2016*, Austin, Tex, USA, October 2016.

[8] M. Vetterli, P. Marziliano, and T. Blu, "Sampling signals with finite rate of innovation," *IEEE Transactions on Signal Processing*, vol. 50, no. 6, pp. 1417–1428, 2002.

[9] Z. Gao, L. Dai, S. Han, C.-L. I, Z. Wang, and L. Hanzo, "Compressive sensing techniques for next-generation wireless communications," *IEEE Wireless Communications Magazine*, vol. 25, no. 3, pp. 144–153, 2018.

[10] J. L. Paredes, G. R. Arce, and Z. Wang, "Ultra-wideband compressed sensing: channel estimation," *IEEE Journal of Selected Topics in Signal Processing*, vol. 1, no. 3, pp. 383–395, 2007.

[11] X. Cheng, M. Wang, and Y. L. Guan, "Ultrawideband channel estimation: A Bayesian compressive sensing strategy based on statistical sparsity," *IEEE Transactions on Vehicular Technology*, vol. 64, no. 5, pp. 1819–1832, 2015.

[12] S. Gishkori, G. Leus, and V. Lottici, "Compressive sampling based differential detection for UWB impulse radio signals," *Physical Communication*, vol. 5, no. 2, pp. 185–195, 2012.

[13] S. Gishkori, V. Lottici, and G. Leus, "Compressive sampling-based multiple symbol differential detection for UWB communications," *IEEE Transactions on Wireless Communications*, vol. 13, no. 7, pp. 3778–3790, 2014.

[14] V. Yajnanarayana and P. Handel, "Joint estimation of TOA and PPM symbols using sub-nyquist sampled IR-UWB signal," *IEEE Communications Letters*, vol. 21, no. 4, pp. 949–952, 2017.

[15] W. Xiong, C. Liu, S. Hu, and S. Li, "High resolution TOA estimation based on compressed sensing," *Wireless Personal Communications*, vol. 84, no. 4, pp. 2709–2722, 2015.

[16] J. Lee, G.-T. Gil, and Y. H. Lee, "Channel estimation via orthogonal matching pursuit for hybrid MIMO systems in millimeter wave communications," *IEEE Transactions on Communications*, vol. 64, no. 6, pp. 2370–2386, 2016.

[17] K. Venugopal, A. Alkhateeb, N. Gonzalez Prelcic, and R. W. Heath, "Channel estimation for hybrid architecture-based wideband millimeter wave systems," *IEEE Journal on Selected Areas in Communications*, vol. 35, no. 9, pp. 1996–2009, 2017.

[18] C. Rusu, R. Mendez-Rial, N. Gonzalez-Prelcic, and R. W. Heath, "Adaptive one-bit compressive sensing with application to low-precision receivers at mmWave," in *Proceedings of the 58th IEEE Global Communications Conference, GLOBECOM 2015*, San Diego, Calif, USA, December 2015.

[19] D. M. Mittleman, "Twenty years of terahertz imaging [Invited]," *Optics Express*, vol. 26, no. 8, pp. 9417–9431, 2018.

[20] J. M. Jornet and I. F. Akyildiz, "Femtosecond-long pulse-based modulation for terahertz band communication in nanonetworks," *IEEE Transactions on Communications*, vol. 62, no. 5, pp. 1742–1754, 2014.

[21] D. L. Donoho, "Compressed sensing," *IEEE Transactions on Information Theory*, vol. 52, no. 4, pp. 1289–1306, 2006.

[22] S. Qaisar, R. M. Bilal, W. Iqbal, M. Naureen, and S. Lee, "Compressive sensing: from theory to applications, a survey," *Journal of Communications and Networks*, vol. 15, no. 5, pp. 443–456, 2013.

[23] Z. Zhang, Y. Xu, J. Yang, X. Li, and D. Zhang, "A survey of sparse representation: algorithms and applications," *IEEE Access*, vol. 3, pp. 490–530, 2015.

[24] J. A. Tropp and A. C. Gilbert, "Signal recovery from random measurements via orthogonal matching pursuit," *IEEE Transactions on Information Theory*, vol. 53, no. 12, pp. 4655–4666, 2007.

[25] L. Wu, X. Wu, and Z. Tian, "Asymptotically optimal UWB receivers with noisy templates: Design and comparison with RAKE," *IEEE Journal on Selected Areas in Communications*, vol. 24, no. 4 I, pp. 808–814, 2006.

[26] L. Yang and G. B. Giannakis, "Optimal pilot waveform assisted modulation for ultrawideband communications," *IEEE Transactions on Wireless Communications*, vol. 3, no. 4, pp. 1236–1249, 2004.

[27] J. M. Jornet and I. F. Akyildiz, "Channel modeling and capacity analysis for electromagnetic wireless nanonetworks in the terahertz band," *IEEE Transactions on Wireless Communications*, vol. 10, no. 10, pp. 3211–3221, 2011.

[28] A. Moldovan, M. A. Ruder, I. F. Akyildiz, and W. H. Gerstacker, "LOS and NLOS channel modeling for terahertz wireless communication with scattered rays," in *Proceedings of the 2014 IEEE Globecom Workshops, GC Wkshps 2014*, pp. 388–392, Austin, Tex, USA, December 2014.

[29] C. Han, A. O. Bicen, and I. F. Akyildiz, "Multi-ray channel modeling and wideband characterization for wireless communications in the terahertz band," *IEEE Transactions on Wireless Communications*, vol. 14, no. 5, pp. 2402–2412, 2015.

[30] J. Kokkoniemi, J. Lehtomaki, K. Umebayashi, and M. Juntti, "Frequency and time domain channel models for nanonetworks in terahertz band," *IEEE Transactions on Antennas and Propagation*, vol. 63, no. 2, pp. 678–691, 2015.